Received: 4 November 2022 | Accepted: 7 November 2022

DOI: 10.1002/rvr2.27

RESEARCH ARTICLE

River IWHR WILEY

Dynamic tracing of fecal bacteria processes from a river basin to an estuary using a 2D/3D model

Guoxian Huang[1] | Roger Falconer[2] | Binliang Lin[3] | Chenghui Xu[1,4]

[1]Chinese Research Academy of Environmental Sciences, Beijing, China

[2]School of Engineering, Hydro-environmental Research Centre, Cardiff University, Cardiff, UK

[3]Department of Hydraulic Engineering, Tsinghua University, Beijing, China

[4]Department of Hydraulic Engineering, Chongqing Jiaotong University, Chongqing, China

Correspondence

Roger Falconer, School of Engineering, Hydro-environmental Research Centre, Cardiff University, Cardiff, CF 243AA, UK.
Email: FalconerRA@cardiff.ac.uk

Funding information

Chinese Joint Fund for water science of National Nature Science Foundation of China, Grant/Award Number: U2240202; Natural Environment Research Council (NERC), UK, Grant/Award Number: GR NE/I008306/1; Major scientific research and development projects of Jiangxi Province, China, Grant/Award Number: 20213AAG01012

Abstract

In this study fecal bacteria processes have been investigated using the EFDC 2D/3D model, based on local refinements using an orthogonal curvilinear grid system and with the model being applied to Ribble river basin, through the estuary, and into the Fylde Coast. The input fluxes from numerous minor rivers and streams within the basin were solved using a grid-based distributed hydrological model (GDHM) and a river network 1D model (RNM1D), developed by the authors. The detailed measured hydrodynamic data, included tide levels and nearshore ADCP 3D velocity field data at four sites and with data being recorded over a 2-week period. During this period continuous monitoring using four types of tracers was also undertaken across the Ribble basin, which included sampling for *E. coli* (*EC*) and Intestinal Enterococci (IE) parameters. Monitoring devices, in the form of buoys, were also used and moved with currents, driven by upstream discharges, tides, waves and wind. The results showed: (i) the grid system gave a detailed topographical representation of the transition zones from the river system to the estuary and coast, with the hydrodynamic and related solute transport processes being well represented; and (ii) the model predicted results fit generally well with the water stage, 3D flow velocity profiles (with some errors in the bottom and surface layers), and *E. coli* concentrations. The tracer paths from the injection sites were simulated using a Lagrangian particle tracking method, which showed that the tracer from the north bank outfalls and the Ribble river could propagate to the highly popular bathing beaches at Blackpool, particularly under the action of South Westerly winds. More detailed solutions and refinements (e.g., wave driven by the wind and density flows caused by different salinities, temperatures, and suspended sediment concentrations) need to be considered in the next stage of this study.

KEYWORDS

bathing waters, estuaries, fecal indicator organisms (FIOs), particle tracking, rivers, three-dimensional modeling, tidal currents

1 | INTRODUCTION

The variation of fecal bacteria, or fecal indicator organisms (FIOs), in shallow regions of river and estuarine systems is generally highly uncertain, due to the significant episodic fluctuations arising as a result of unsteady sources and delivery from catchments (Bussi et al., 2017), together with the multiple inner driving stresses within the system (de Brauwere et al., 2014). These highly episodic events frequently cause bathing beaches to be closed, especially where high concentrations of *E. coli* (EC) and/or intestinal enterococci (IE) occur. However, it is often difficult to predict these processes due to a number of limitations in the data and process representations, including: (i) a shortage of detailed continuous high frequency monitoring data, related to flow velocity, sediment and FIO concentrations and flux inputs from rivers and waste water outfalls, and so forth. around beaches; (ii) accurate numerical model predictions of the wetting and drying of inter-tidal mudflats and habitats and the corresponding mass transport of fluid and solute processes in these shallow regions, even using highly refined 2D/3D models; (iii) the local FIO sources from birds and so forth. along beaches and remobilization of previous accumulated FIOs by rainfall, waves and winds. Unfortunately, these variables are often the most influential covariates across all models and are important in enhancing model accuracy (Cyterski et al., 2022; Kim et al., 2021).

In river and estuarine basins, the hydrodynamic process are often highly complex (Seo et al., 2022), and are driven by complex bathymetries, with pronounced spatiotemporal heterogeneity in the bottom roughness and often caused by: nonuniform sediment particles and salt marshes with different plants, unsteady upstream inflows, tide and wave processes from the open sea, wind-driven currents, and density driven currents caused by turbidity, temperature and salinity differences, especially in deltaic zones between rivers and estuaries (Arevalo et al., 2022; Horner-Devine et al., 2015). These complex hydrodynamic flow fields can cause complex transportation pathways of passive pollutants, such as fecal bacteria or FIOs (Abu-Bakar et al., 2017; Huang et al., 2017; King et al., 2021). Likewise, along the coast there are generally sand beach regions, where numerous outfalls from sewage and riverine confluences often discharge untreated fecal bacteria, resulting in high concentrations and fluxes of FIOs along bathing beaches. These FIO inputs into the bathing waters are difficult to measure quantitatively and are equally difficult to model, with the need to include outfall inputs (often diffuse), riverine inputs (including both source and diffuse inputs) and resuspension of contaminated sediments from the river bed, caused by the dynamic coupling between the FIOs and suspended sediment particles (Gao et al., 2011). These inputs and interactive processes are often further complicated by large variations in wind magnitudes, wind directions, and turbulence and stratification effects. In acquiring data for such model predictions, the tracer release studies are generally required from different sites, with the objective being to monitor the key transport of FIOs, including the processes of dispersion and diffusion. However, it is often difficult to cover the full range of sampling required by limited field experiments, where such tracer releases often have to be undertaken, particularly where safety risks are involved and especially during high spring tides at night. The integration of tracer releases, and the monitoring and analyses of hydro-bacterial field data, along with numerical model simulations provides a useful tool to quantitatively determine pathway and concentrations of FIOs from high concentration inputs, both point and diffuse sources, into river basins and then into estuaries and coastal bathing waters.

These complex hydro-biological processes induce further challenges to numerical model simulations of both the hydrodynamic and the related solute transport processes in river, estuary and coastal systems, especially in regions of stability for solute mass and momentum conservation, as well as producing accurate predictions across highly varying spatial scales and grid sizes through rivers and estuaries (de Brauwere et al., 2014). First, the grid distribution and generation is one of the key issues in numerically modeling the complex hydrodynamic and solute mass transport processes, especially for: irregular boundaries, significant differences in scales and complicated topographies. A curvilinear grid system is beneficial in fitting irregular boundaries and involves less calculations compared to rectangular grid systems in treating river and estuarine boundaries, particularly in the vertical plane. Some software and open source codes, such as Deft3D, EFDC, and so forth, use curvilinear grid systems. In refining these tools further attention needs to be paid to the treatment of local dense grid variations, especially in narrow channels and from shallow to deep transition zones or vice versa, where local rapid water depth changes and irregular boundaries may decrease the mass and momentum conservation level in predicting the hydrodynamic and solute transport processes, particularly in dry seasons or during low tidal levels. In considering such complex river and estuarine boundaries, the hydrodynamic and solute transport processes in the model domain have been simulated using the EFDC 2D/3D model, with a curvilinear grid configuration, and setup and refined for the Ribble river basin and estuary, the Fylde Coast, Liverpool Bay and part of Irish Sea. The corresponding 3D model predicted water levels and tidal river induced currents were validated using measured data acquired at several monitoring sites. Finally, by using a depth averaged version of the 3D model, including wind effects, a Lagrangian particle tracking method was included to determine more accurately the trajectory of tracer propagation and concentration distributions (Li et al., 2022; Simantiris et al., 2022). In addition, the refined EFDC 3D model has been tested for its accuracy in predicting the hydrodynamic and solute transport processes at multiple scales within the Ribble river and estuarine system, which includes complex and dynamic boundaries, with the model being refined to predict *E. coli* dynamics, particularly in the shallow depths (typically 0.4 m) of the bathing water beach regions and with inputs of fecal bacteria being included from a range of sources.

2 | MATERIALS AND METHODS

2.1 | Study area and data

The coastal basin domain included the several river and estuarine basins, with irregular boundary shapes and a complex topography. The basin included 11 main rivers, namely the Clwyd, Dee, Mersey, Ribble, Darwen, Douglas, Wyre, Lune, Kent, Leven, and Duddon, they all flows into the Irish Sea. In the transition region between the rivers and the Irish sea, there are some relatively large estuaries, including the Duddon, Morecambe, Ribble, Mersey, and Dee estuaries, where intense mixing of the dilute water, suspended sediments and related pollutants take place as a result of the strong tides from the outer Irish Sea and input flows, with different concentrations and temperatures, together with the irregular bank boundaries and complex bathymetries in these rivers and estuaries. The model domain, including the estuaries, was 9664 km^2. There are 29 national bathing beaches in the coastal model domain and a shellfish harvesting area located in the Ribble estuary, with both required to meet the standards set out in the EU Bathing Water Directive 2006/7/EC, Shellfish Waters Directive–2006/113/EC. The main data collection used in the model system included: (i) detailed topographic data acquired from different sources, (ii) sediment particle sizes in the rivers and estuarine beds, with these data being used to estimate the bed roughness; (iii) hydrological and hydrodynamic data, including inflow discharges and ADCP measurements at four different monitoring sites; and (iv) tracer concentration monitoring data within the river Ribble and the estuarine region.

2.2 | Methodology

2.2.1 | Hydrodynamic measurements

The hydrodynamic measurement, including tidal levels and 3D velocities, were recorded using Acoustic Doppler Current Profilers (ADCP) at four (L2~L5) monitoring sites (see Figure 1), along the Fylde Coast, from November 2013 to January 2014. These measurements were carried out by Fugro EMU limited, through a contract with the Centre for Research into Environment and Health (CREH), at the University of Aberystwyth, and as part of the Cloud to Coast (C2C) Project.

2.2.2 | Tracer releasing and field monitoring

The two tracer releasing and field monitoring was carried out along the Ribble river and estuary, with the data being acquired by CREH, University of Aberystwyth, also as part of the Cloud to Coast (C2C) Project. The tracer injection included 10^{16}–10^{17} organisms, which is the equivalent of about 1~67 million cubic meters of storm sewage. The tracer types included Phi-X174, *Enterobacter cloacae* phage, Serratia marcescens phage and Coliphage MS2. In total, there were two tracer injections and monitoring programmes; the first injection was on September 8, 2013, and the second injection was on October 21, 2013. Hourly sampling was carried out up to 48 h and 56 h across the sites, with the tracer being tracked using a boat, which cover the four tidal cycles. The detailed information about tracer measurement is given in Table 1 and Figure 1.

2.2.3 | Modeling system for the hydrodynamic and FIO processes in the river-estuarine basin

To guarantee the reasonable solution of mass transport in the narrow and deep river channel and acquire a relatively high calculation efficiency across the whole domain, the grid was refined based on the following criteria: (i) the ratio between the maximum and minimum edge for two adjacent cells was less than 3.0; (ii) the narrow riverine region where the grid length was generally less than 10.0 m and the grid size near the Irish sea was close to 600 m where the related sediment and bacteria concentrations were very small; and (iii) the total number of cells within the grid system was about 40,000 orthogonal curvilinear cells. The different topographic data was measured by cross-section sampling in the upper reaches of the rivers Wyre, Douglas and Ribble and with the data being interpolated using new methods (Huang et al., 2014). Likewise, the topographic data near the sandy bathing beaches of Blackpool and Morecambe Bay, and in the Ribble and Dee estuaries were acquired from LIDAR data with a 3–10 m sampling range. The EFDC2D/3D code was used to study the hydrodynamic, sediment transport and FIO processes in a river, estuarine and coastal system, from the catchments to the coast. The detailed methods for grid generation, topography interpolation, bed sediment particles, bottom roughness setup are given in the references (Huang, Falconer, Boye, et al., 2015; Huang et al., 2017).

2.2.4 | Flow, suspended sediment, and *E. coli* concentrations

The discharge, suspended sediment, and *E. coli* concentrations from the 11 main rivers were obtained from the measured data, and the related data from other minor rivers and outfalls, were predicted using the grid based hydrological model (GBHM) (Huang, Falconer, Lin, et al., 2015). These measured and predicted data were included in the one dimensional river networks model for the hydrodynamic, suspend sediment and water quality process predictions for multiple stagnation points and multiple flow directions (RNM1D) (Huang et al., 2018), with encouraging validation and verification results being obtained in the study domain when the measured data is limited.

2.2.5 | Trace modeling using Lagrangian particle tracking model

Based on the depth averaged 3D hydrodynamic model results, the Lagrangian particle tracking 2D model was used, which included the simulation of the transport and diffusion of four tracers in the river and coastal basins. Since the tracers have approximately the same density as water, and can rapidly dilute in water, it can be seen that the tracer moves synchronously with the river coastal

FIGURE 1 Tracers releasing processes and field monitoring positions

currents. Therefore, the particle position at the next time step in the horizontal plane in the model can be calculated using the following equation giving:

$$X(t+\Delta t) = X(t) + \int_t^{t+\Delta t} V_t \, dt + \Delta\alpha \tag{1}$$

where $X(t)$ and $X(t+\Delta t)$ are the positions at times t and $t+\Delta t$ respectively, V_t is the transport velocity of the tracer, $\Delta\alpha$ is the length of tracer's random movement driven by the turbulent flow, which is calculated using the following equation:

$$\Delta\alpha = R\sqrt{6K_\alpha \Delta t} \tag{2}$$

where R is a random data range from −1 to 1, and K_α is the diffusion coefficient in the horizontal direction, which is obtained from the 2D and 3D models.

TABLE 1 Position of the microbial tracer releases and injection times

Tracer	Released from	Release time of microbial tracer Greenwich Mean Time	Tracer titer (pfu/ml)	Volume (L)	No. organisms released	Latitude °N	Longitude E/W
Phi-X174	Fairhaven CSO (Combined Sewere Overflow) outfall	2013-09-08 12:59	2.0E + 12	5	1.00E + 16	53.726253	−3.008819
Enterobacter cloacae phage	River Douglas at Ribble confluence	2013-09-08 13:32	8.3E + 12	5	4.15E + 16	53.734348	−2.857292
Serratia marcescens phage	Southport WwTW (Waste water Treatment Works) outfall	2013-09-08 12:44	5.0E + 12	5	2.50E + 16	53.680830	−2.952743
Coliphage MS2	Manchester Square CSO outfall	2013-09-08 07:15	1.9E + 14	5	9.50E + 17	53.807424	−3.071043
E. cloacae phage	Preston WwTW outfall	2013-10-21 13:00	4.5E + 13	5	2.25E + 17	53.744349	−2.827119
Serratia marcescens phage	River Darwen, Blue Bridge	2013-10-21 12:50	3.5E + 12	5	1.75E + 16	53.744544	−2.662027
Coliphage MS2	Harrowside CSO outfall	2013-10-21 12:58	1.3E + 14	5	6.50E + 17	53.783733	−3.067933

3 | RESULTS

3.1 | Verification of hydrodynamics in the estuarine region

Verification of the tidal levels at the L2~L5 monitoring sites (see Figure 2b) are showed in the Figure 3, based on the model results. The predicted tidal levels agree well with the measured data in terms of both the tidal magnitude and phase. The predicted water levels are about 0.2 m lower than the measured values at low ebb tide and during flood tide rising and falling is about 1.0 h ahead and behind the measured data. This error is thought to be caused by the low tidal boundaries value, calculated from the Mike global model, and the dynamic wave process being omitted in the model system. It is recommended that more mechanism processes about the wave and sensitivity test analysis in the parameter adjustment should be included in any future studies.

The monitoring frequency of the current velocity in the x, y, and z directions using the ADCP data with the data being gathered every 10 min along the 18–35 vertical layers at sites L2~L5, which gives the highly dynamic and complex variations in the 3D hydrodynamic field nearshore area. The current structure is mainly significantly governed by the topography of river-estuarine system and driven by the tide, wave, wind, river inflow discharge, density flow in the delta zone and the currents from offshore. In considering the data integrity, the measured velocity magnitude at the different vertical layers at the L3–L5 sites, are compared with the predicted results from the EFDC3D model and are shown in Figure 4 at a specific time. The results shows: (i) the flow predicted velocity profiles using the EFDC model fitted generally well with the measured data when the measured velocity profiles are generally logarithmic or parabolic in shape, as shown in Figure 4 and with the calculated error range being ±0.15 m/s, (ii) there are relatively large prediction errors occurring when extreme velocity magnitudes occur near the free surface (e.g., L3(c)) and the maximum value near the bottom layer, which may be driven by large winds and strong density currents driven by the water mass having different concentration in salinity and suspended sediments, respectively. In addition, the irregular boundaries near the river delta zone may also play an important role in the current mixtures and irregular vertical velocity profiles.

3.2 | Verification of velocities and concentrations from the tracer injection point

Tracer release in the model is taken as being a point source, with the additional flow from the discharge point boundary being estimated by the injection volume and injection time. The temporal process of the measured surface velocity magnitude is calculated at different coordinate positions of the moving buoy at a given time and the predicted velocity near the surface layer is calculated from the EFDC 3D

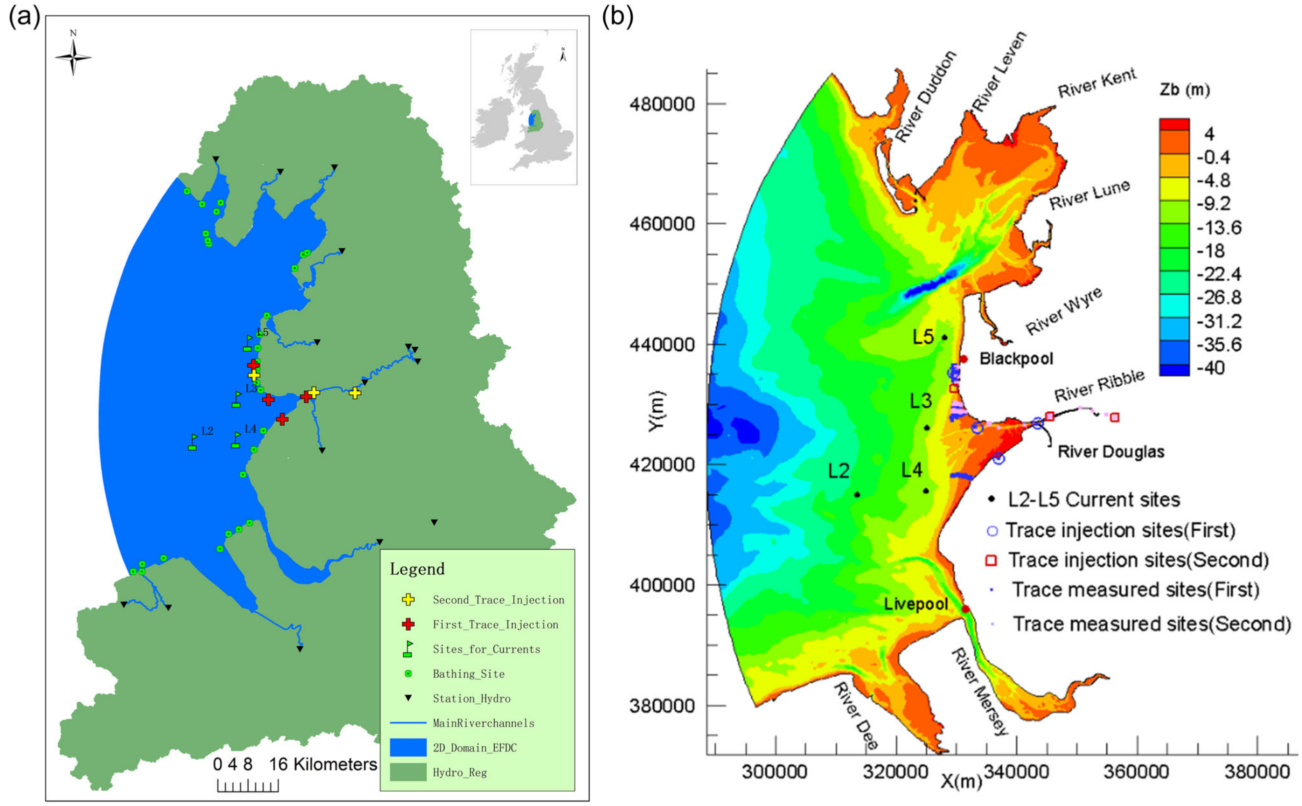

FIGURE 2 (a) Model domain, and (b) topography and key positions of the river and estuarine inputs

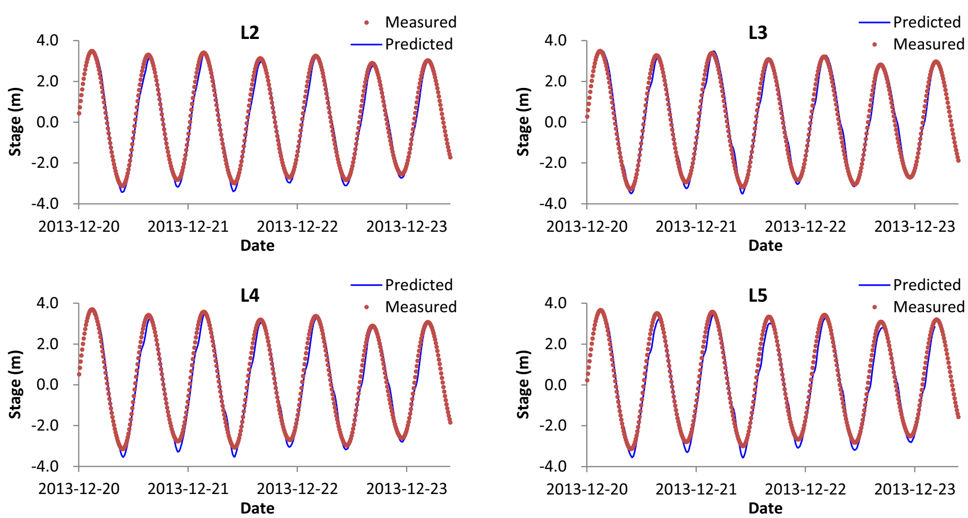

FIGURE 3 Verification results for tidal levels at the L2~L5 monitoring sites

model. Meanwhile, the related tracer concentration is measured at a range of points.

The tracer movement and concentration, as well as the local *E. coli* concentration, are all measured by floating balls, which moved with the local currents near the bathing beaches and at the monitoring sites: Sport_407, St_An_408, and St_An_409 and so forth. The measured velocity of the floating balls was estimated by the distance moved over a given time duration. The predicted velocity at the surface layer from the EFDC model were then estimated at the monitoring sites, based on interpolated velocity outputs from the 3D model at the monitoring times and positions.

In total, from the Figure 5, it can be seen the model predicted velocities and tracer concentrations generally fitted well with the measured data, especially at the sites in relatively deeper water. The errors in the surface velocity calculations in the shallower beach sites were expected to be larger than those measured and predicted in deeper zones due to the varying predictions in the wetting and drying

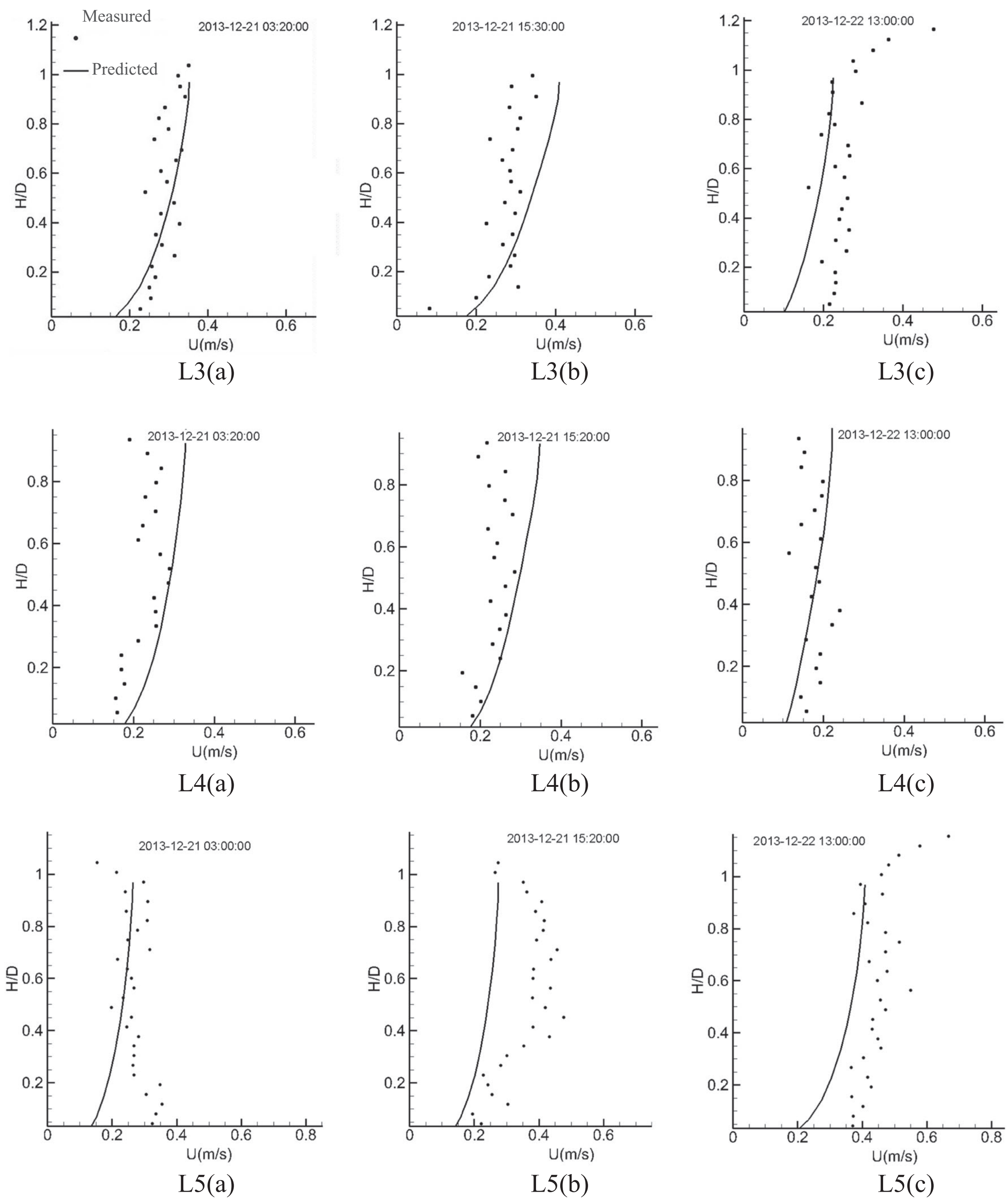

FIGURE 4 Velocity magnitudes over depth at sites L3~L5

algorithm, the abrupt mesh size variations in the vertical direction and the difficulty in predicting the hydrodynamics accurately at a point in shallow water. Therefore, the tracer and *E. coli* concentrations at these points were expected to be more affected by the accuracy of the hydrodynamic predictions at the site, relative to comparable concentrations measured and predicted in deeper water. In addition, our previous 2D modeling showed that the predicted *E. coli* concentrations with suspended sediment coupling were higher and closer to the measured data than the related values without suspended sediment coupling (Huang et al., 2017). In the current study sediment and *E. coli* coupling was not coupled in the 3D model. Subsequent developments are needed to undertake the next step in qualifying quantitatively the difference under the local dense grid density around the beaches, the driving forces of the complex wind fields, coupling of graded suspended sediment transport and dynamic variations in the decay rate under different hydro-environmental conditions. Moreover, some advanced software or open source code for the hydrodynamics, trace, and *E. coli* transportation predictions, with an unstructured grid system such as MIKE21 and 31 or Telemac 2D and 3D could be used for comparative research purposes, with the same parameters

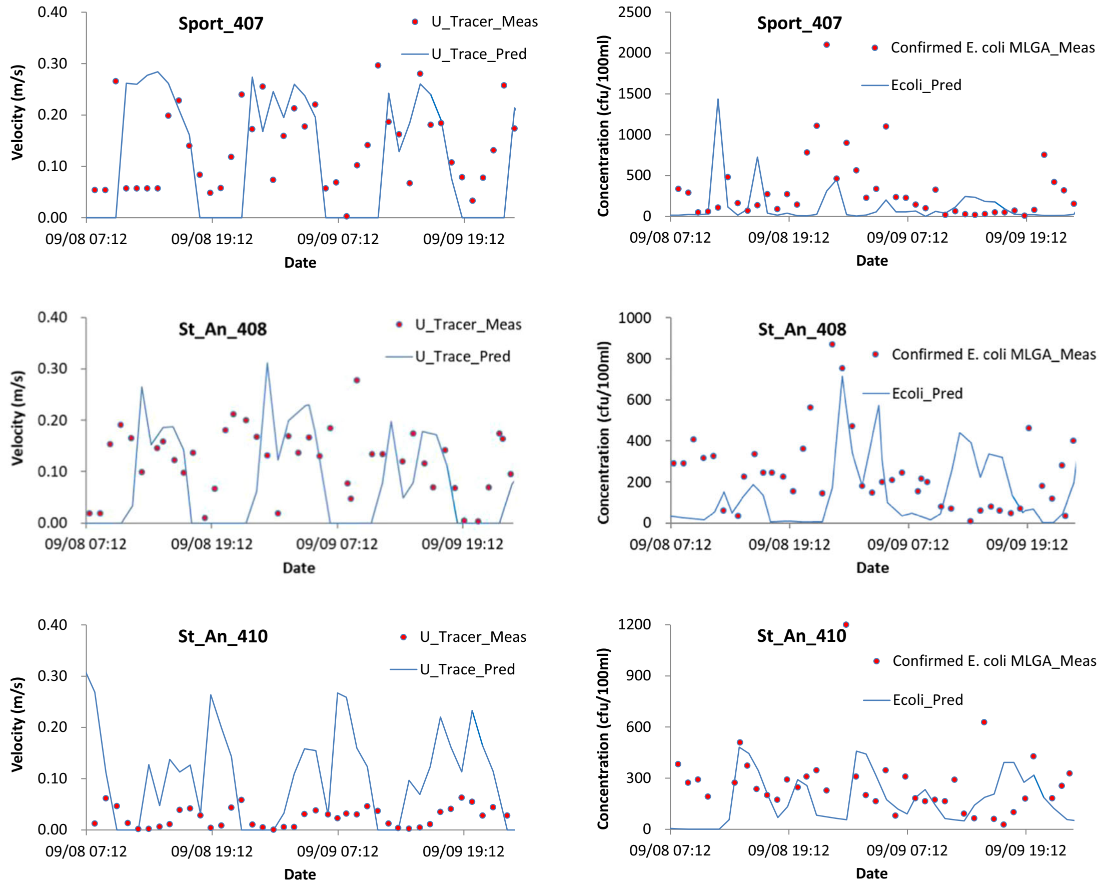

FIGURE 5 Comparison of tracer estimated and model predicted velocities and concentrations

included in the model and with the aim of reducing the uncertainty in the model predictions.

3.3 | Tracer simulations in the river Ribble and estuarine system under the action of different winds

After solving the tidal current field using the 3D model, the moving path of the tracer was solved using the depth averaged velocity field and using a Lagrangian particle tracking method to track the tracer at every time step. In this model study, the tracer was first setup in the cell in which the injection sites were located and the tracer was assumed to be contained just in this cell at the given starting time. Model simulations were then undertaken for different wind velocities, including speed with 2 m/s and different directions, with the wind effects being coupled to the prediction of the particle movement. The corresponding results are given in Figure 6.

The complexity of the flow field driven by the multiple stresses in the delta region of the Ribble estuary makes the complex projectile paths very different for different injection sites (see Figure 6). Due to the processes of advection and diffusion, the path of a tracer from the same injection site may appear very different for local wind directions and so forth. The shape of the tracer plume may be expanded, distorted, broken, decomposed, and re-merged by the processes of advection and dispersion and interaction with the winds. The numerical model predictions show that the modeling system can be used to simulate the dynamic variation in tracer advection and diffusion and the related positions, per time step, driven by the different controlled processes and stresses. This case study shows that there is an obvious difference in the spatial distribution of tracer in the delta zone of the Ribble estuary at 10–20 h after the time of injection of the tracer (see Figure 6b [I] and [II]). The difference is mainly driven by the different NW and SW wind directions, together with a nonuniform spatial distribution of the velocity field in the river delta. After 36 h post tracer injection, different tracers from different injected sites were mixed as a result of the tidal currents and winds, with the spatial tracer plumes in the horizontal plane being distorted and broken up in the head of the river delta, where there is a complicated deltaic fan-type structure in the bed topography distribution and correspondingly in the hydrodynamic conditions (see Figure 6cI,II). After 46 h, the tracer plumes from the Ribble estuary tend to form a stable shape, and different wind directions cause obvious differences in the spatial distribution of the tracer particles (see Figure 6dI,II). The NW winds tend to drag the currents, tracer plumes and

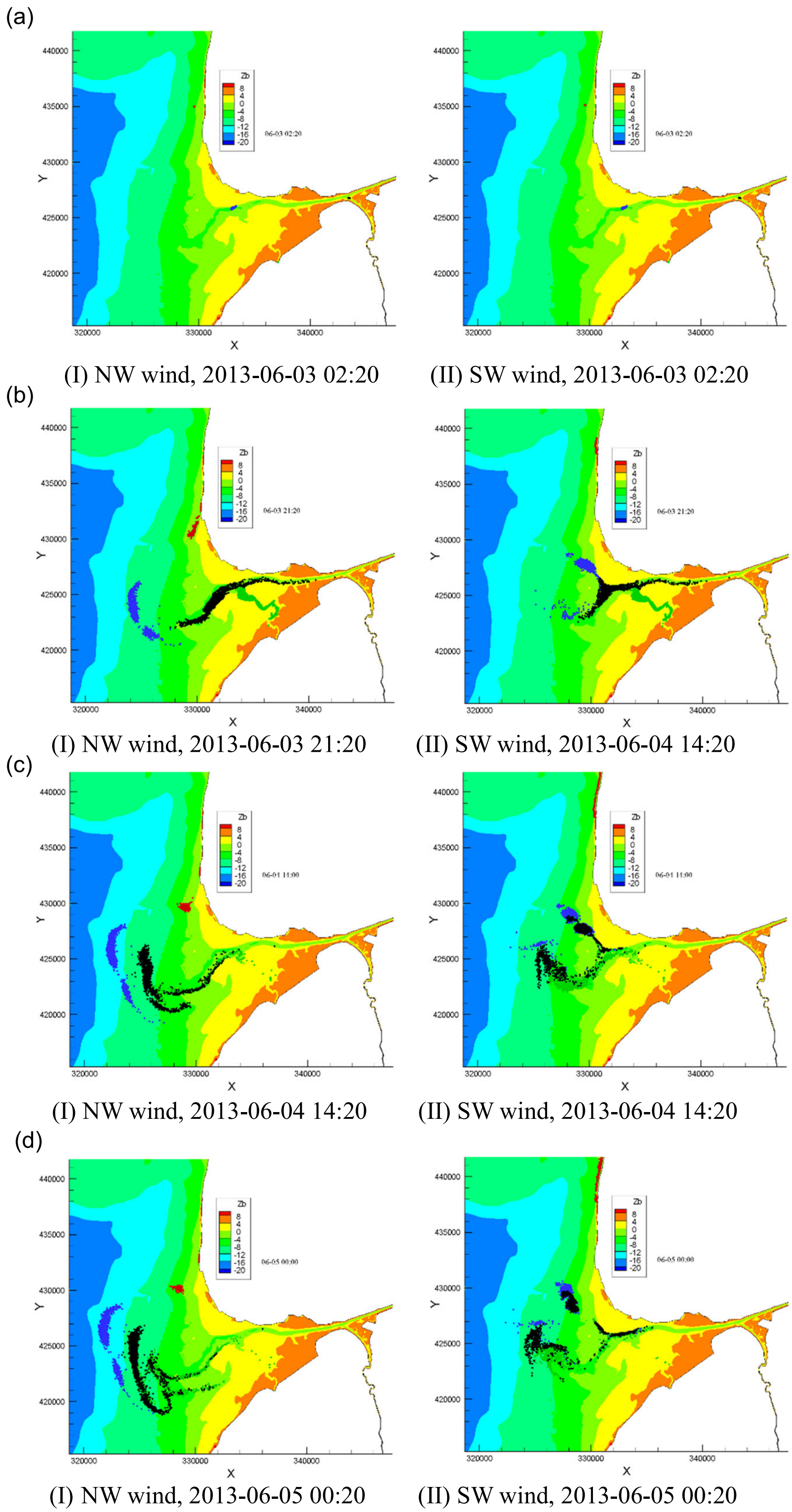

FIGURE 6 Spatial distribution of traces at the different time injected at four sites moving with NW and SW wind with velocity magnitude 2.0 m/s

FIO concentrations from the river Ribble to the nearshore of south bank of estuary. In contrast, the SW winds tend to drag the currents, tracer plumes and FIO concentrations to the North bank. The tracer and FIO releases from the North bank outfalls tend to move along the Blackpool beaches, which tends to cause higher FIO concentrations in the region and thereby leading to local water quality risks of noncompliance with the required EU Bathing Water standards.

Moreover, the ADCP measurement results at the L2–L5 sites show that the flow velocity in the Ribble estuary has intense temporal variations and significant 3D features, and will not be reasonably represented using typical profiles of the logarithmic or parabolic distribution function in the velocity distribution along the vertical axis. Therefore, for more accurate predictions of the hydrodynamics including wind conditions in the estuary would be better represented using a 3D model. Such a model would also give a better representation of the advection and dispersion of different pollutants or tracers, particularly when different densities, and dynamic linkage between these pollutants and the bed and suspended sediments are included.

4 | DISCUSSION AND CONCLUSION

4.1 | Mechanisms and modeling of FIO process from catchments to coast

The mechanisms and related modeling of FIO processes from catchments to the coast, include some sections as production accumulation, releasing, delivery and decay process, and so forth. The FIO processes within the water column are driven by multiple factors (Cho et al., 2016; Kay et al., 2005), in which: rainfall, radiation, sediment particles, and land use (Crowther et al., 2002), all play some important roles in FIO transport from catchments to coast (Kashefipour et al., 2006; Perkins et al., 2016). There are various studies that have been undertaken by various authors in the catchments (Huang, Falconer, Lin, et al., 2015), rivers (Huang et al., 2018) and the estuary (Boye et al., 2015; Huang et al., 2017; Lin et al., 2008) for the Ribble river basin and Fylde coast. In this paper, the FIO transportation processes and related tracer movements in the Ribble river basin and estuary have been the focus of investigation in the 3D hydrodynamic flow field, with the complex FIO processes being driven by multiple processes, including, for example, the 3D velocity distribution and the wind speeds and directions. A quantitative evaluation of the distribution and concentration of FIOs has been undertaken, driven by the FIO sources from adjacent outfalls, riverine inputs and different transportation pathways for different weather, hydrological, and environmental conditions.

Aspects of these processes are partly explained, based on the series of limited field monitoring data for the currents and different FIOs and tracer concentrations for different injection locations and measurements through the work of various members of the C2C project and authors of the refined 2D and 3D numerical model studies. The high frequency of the current measurement results showed that the vertical profiles of velocity changed rapidly under multiple stresses and processes. The vertical velocity profile did not always fit well with a typical logarithmic or parabolic vertical velocity profile. The peak velocity magnitude should theoretically appear near the flow surface. However, in the current study the maximum velocity value occasionally appeared nearer to the bed layer. The irregular profiles were influenced by the large winds, strong mixing, stable stratification and density current intrusion, induced by different concentrations in salinity and suspended sediments from the upper reach of the estuary to offshore. Furthermore, the irregular boundaries in the estuary would have also played an important role in affecting the velocity field, both in terms of the horizontal velocity field and the irregular vertical velocity profiles. These irregular vertical velocity profiles had an impact on the sediment and FIOs transport processes, which further increased the difficulty in validation and verification of the 3D hydrodynamic model, due to the simplification of some important stress terms and particularly the bed, surface and turbulent stresses through the water column.

In addition to the complicated hydrodynamic system, the measured velocity close to the bed layer or free surface layer showed a large variation in the Ribble estuary and in coastal zone around the estuary. The relative sparse sampled data in the near bed and surface layers did not show such large variations as predicted. The relative larger measurement errors and uncertainty in the near bed data using the ADCP was primarily attributed to the relatively high suspended sediment concentrations near the bed layer, which in turn weakened the transmission and reception of the acoustic wave instrument.

Furthermore, the complex transport pathways for the FIOs and tracer concentrations included parts of the estuary where recirculating flows occurred, particularly in the shallow beach regions where wetting and drying occurred, in addition to the linked regions where narrow and deep ditches or pipes from outfalls discharged into the river and estuarine basins. In addition, the adsorption and desorption coupling between bed and suspended sediment particles, FIOs and tracers are complex and still not well understood. Furthermore, the shielding of solar radiation through high suspended sediment levels also reduced the decay and mortality of FIOs.

4.2 | Errors in FIO concentrations and tracer paths associated with numerical model predictions

Based on the predicted results and analysis of the complexity of FIO processes, a 3D hydrodynamic and FIO model is required to predict the velocity and concentration distributions in 3D flow structures. The reasonable spatial resolution and terrain representation included in the model's grid system needs to be strengthened, especially in the areas of complex bathymetries, as in the Ribble estuary, where sand beaches and narrow ditches are linked through outfalls to open water. Such improvements will enhance mass conservation, and improve the accuracy in predicting the transport of FIOs. Our results showed that the wind played an important role in the tracer plume trajectories and a SW wind advected the tracer plume and high FIO concentrations from Ribble estuary and adjacent outfalls to the Fylde Coast and particularly Blackpool beach. This trajectory of the plumes flowing out of the estuary might lead to the noncompliant high FIO concentrations along Blackpool beach.

In considering the relatively large variations and related calculated discrepancies in the vertical velocity profiles, and the 2D solution of the tracer plume trajectories based on the depth averaged model results of predicted 3D velocity fields also contributed to errors in the model predictions. In addition, the physical processes associated with wind induced waves, water temperature variations and salinity differences all affected model parameters and should be further refined in future model simulations. Bed and suspended sediment particles also provide an important mechanism for the transport and survival of FIOs and the current research study reported herein showed that coupling the suspended sediments and FIOs in the 2D model noticeably enhanced the predicted accuracy of the FIO concentrations and particularly along the beaches (Gao et al., 2011; Huang et al., 2017). In the 3D model, the graded sediment particles would also be coupled during simulations to the FIOs and related tracers. The differences in the FIO centration and tracer plume trajectories and key process representations for high concentrations of FIOs would be affected by a combination of wind, tide and velocity values, together with the input values of FIO and sediment concentrations; all of which need to be checked against field data. Furthermore, the probability of high concentrations of FIOs along beaches need to be analyzed using a series of model scenarios for calculations as a next step.

4.3 | Decay rate of *E. coli* for different conditions

Following the setup of a well calibrated and validated model in terms of predicting the key hydrodynamic processes in a river and estuarine basins, the advection, dispersion and decay of FIOs in the basin is the next key step, with these parameters often having a relative large variation in concentration predictions for a wide range of environmental conditions. The decay rate for fecal bacteria is normally expressed in terms of the T_{90}, which is the time length for a death rate of 90%. In the modeling system reported herein, the T_{90} value is set according to the values obtained from field data acquired by the Centre for Research into Environment and Health (CREH), at Aberystwyth University (https://www.sheffield.ac.uk/c2c). The T_{90} values used in the present EFDC 3D model were the same as the values used in a previous paper used by the authors in the EFDC 2D model (Huang et al., 2017). The T_{90} value varies dynamical and primarily with: radiation, sediment properties and concentration, salinity and temperature, with this parameter being a key coefficient in the modeling predictions of the FIO concentrations along the river basin reach. The value of the T_{90} decay rate for fecal bacteria were obtained through extensive laboratory analysis, following field data acquisition and numerical model tests. The decay rate of the fecal bacteria played an important role in the predictive model results (Sagarduy et al., 2019) and led to a range of predicted results in the concentration, flux, and microbiological potential risk (Bonamano et al., 2015). A uniform formula for the decay modification has been developed for inclusion in the existing models, which is dependent on a range of different factors, including: sediment setting velocity, water depth, solar radiation, water temperature and so forth. (Lubo et al., 2006). An extensive review of fecal bacteria decay and the dependence on key factors in the analysis as given in the work of (Weiskerger & Phanikumar, 2020). The widely used equation for the T_{90} related value and its dependency on a range of key parameters, including: light intensity, water depth, suspended sediment concentrations and so forth. varies over a large value range from 2 h to 100 h (Guillaud et al., 1997). Meanwhile the T_{90} also varies with salinity and limited organic matter loading (Ekaterini, 1997), with model tests in Norway showing that the value of the decay rate, with wind effects, had an important influence on the *E. coli* concentration processes at compliance sites along Norwegian beaches (Eregno et al., 2018).

5 | CONCLUSIONS

In the study reported herein a 3D model has been refined and built to predict the hydrodynamic, suspended sediment and FIO processes based on the widely used EFDC 3D model. The depth averaged hydrodynamic and solute transport model was then used, based on the 3D model predictions, to drive a tracer concentration discharge from a point source using a Lagrangian particle tracking method. The measured tidal levels velocities were used to calibrate and verify the hydrodynamic process, with the model results generally agreeing well with measured data, except for the relative large errors in the surface and bottom layers during specific simulation periods. These findings showed that the model needed to include some further improved process representations, including driving forces and related parameters, to deliver improved predictions. The prediction of the tracer plumes under the action of SW and NW winds along the Fylde coast beaches showed that the wind direction had a significant impact on the high FIO concentrations along the Fylde coast and Blackpool beach. The studies reported herein showed that a solution of the high FIO concentrations along the bathing beaches showed that the impact of high FIO values along the bathing beaches were governed by inputs form several different outfalls. Further work is needed to supplement the decay rate test, coupling between the sediment transport and FIOs dynamics, probability analysis for high concentrations of FIOs along the main beaches through a series of scenario simulation of refined and well verified model predictions.

ACKNOWLEDGMENTS

The research reported herein was funded by the Natural Environment Research Council (NERC), UK (GR NE/I008306/1) and the Chinese Joint Fund for water Science of the National Nature Science Foundation of China (GR No. U2240202), Major scientific research and development projects of Jiangxi Province, China (GR No. 20213AAG01012). The authors are also grateful to the Environment Agency North West for their provision of data and to all colleagues from the universities of Aberystwyth, led by Professor David Kay, and Sheffield, who also worked on the NERC C2C project. The tracer data reported in this study were collected and analyzed for the Cloud to Coast Project by the Centre for Research into Environment and Health (CREH), University of Aberystwyth.

DATA AVAILABILITY STATEMENT

The data in the manuscript can be applied by writing the email to the first author with the reasonable reasons.

ETHICS STATEMENT

The authors confirm that this article does not contain any studies with animal or human being.

ORCID

Guoxian Huang http://orcid.org/0000-0002-4418-9250

REFERENCES

Abu-Bakar, A., Ahmadian, R., & Falconer, R. A. (2017). Modelling the transport and decay processes of microbial tracers in a macro-tidal estuary. *Water Research*, *123*, 802–824.

Arevalo, F. M., Álvarez-Silva, Ó., Caceres-Euse, A., & Cardona, Y. (2022). Mixing mechanisms at the strongly-stratified Magdalena River's estuary and plume. *Estuarine, Coastal and Shelf Science*, *277*(108077), 108077.

Bonamano, S., Madonia, A., Borsellino, C., Stefanì, C., Caruso, G., De Pasquale, F., Piermattei, V., Zappalà, G., & Marcelli, M. (2015). Modeling the dispersion of viable and total *Escherichia coli* cells in the artificial semi-enclosed bathing area of Santa Marinella (Latium, Italy). *Marine Pollution Bulletin*, *95*(1), 141–154.

Boye, B. A., Falconer, R. A., & Akande, K. (2015). Integrated water quality modelling: Application to the Ribble Basin, U.K. *Journal of Hydro-environment Research*, *9*(2), 187–199.

de Brauwere, A., Gourgue, O., de Brye, B., Servais, P., Ouattara, N. K., & Deleersnijder, E. (2014). Integrated modelling of faecal contamination in a densely populated river–sea continuum (Scheldt River and Estuary). *Science of the Total Environment*, *468–469*(0), 31–45.

Bussi, G., Whitehead, P. G., Thomas, A. R. C., Masante, D., Jones, L., Jack Cosby, B., Emmett, B. A., Malham, S. K., Prudhomme, C., & Prosser, H. (2017). Climate and land-use change impact on faecal indicator bacteria in a temperate maritime catchment (the River Conwy, Wales). *Journal of Hydrology*, *553*, 248–261.

Cho, K. H., Pachepsky, Y. A., Oliver, D. M., Muirhead, R. W., Park, Y., Quilliam, R. S., & Shelton, D. R. (2016). Modeling fate and transport of fecally-derived microorganisms at the watershed scale: State of the science and future opportunities. *Water Research*, *100*, 38–56.

Crowther, J., Kay, D., & Wyer, M. D. (2002). Faecal-indicator concentrations in waters draining lowland pastoral catchments in the UK: Relationships with land use and farming practices. *Water Research*, *36*(7), 1725–1734.

Cyterski, M., Shanks, O. C., Wanjugi, P., McMinn, B., Korajkic, A., Oshima, K., & Haugland, R. (2022). Bacterial and viral fecal indicator predictive modeling at three Great Lakes recreational beach sites. *Water Research*, *223*(118970), 118970.

Ekaterini, T. (1997). Growth possibilities of *E.Coli* in natural waters. *International Journal of Environmental Studies*, *52*(1), 67–73.

Eregno, F. E., Tryland, I., Tjomsland, T., Kempa, M., & Heistad, A. (2018). Hydrodynamic modelling of recreational water quality using *Escherichia coli* as an indicator of microbial contamination. *Journal of Hydrology*, *561*, 179–186.

Gao, G., Falconer, R. A., & Lin, B. (2011). Numerical modelling of sediment–bacteria interaction processes in surface waters. *Water Research*, *45*(5), 1951–1960.

Guillaud, J. F., Derrien, A., Gourmelon, M., & Pommepuy, M. (1997). T90 as a tool for engineers: Interest and limits. *Water Science and Technology*, *35*(11), 277–281.

Horner-Devine, A. R., Hetland, R. D., & MacDonald, D. G. (2015). Mixing and transport in coastal river plumes. *Annual Review of Fluid Mechanics*, *47*, 569–594.

Huang, G., Falconer, R. A., Boye, B. A., & Lin, B. (2015). Cloud to coast: Integrated assessment of environmental exposure, health impacts and risk perceptions of faecal organisms in coastal waters. *International Journal of River Basin Management*, *13*(1), 73–86.

Huang, G., Falconer, R. A., & Lin, B. (2015). Integrated river and coastal flow, sediment and *Escherichia coli* modelling for bathing water quality. *Water*, *7*(9), 4752–4777.

Huang, G., Falconer, R. A., & Lin, B. (2017). Integrated hydro-bacterial modelling for predicting bathing water quality. *Estuarine Coastal & Shelf Science*, *18*, 145–155.

Huang, G., Falconer, R. A., & Lin, B. (2018). Evaluation of *E.coli* losses in a tidal river network using a refined 1-D numerical model. *Environmental Modelling and Software*, *108*, 91–101.

Huang, G., Lin, B., Zhou, J., & Falconer, R. A. (2014). A new spatial interpolation method based on cross sections sampling. *11th International Conference on Hydroinformatics (HIC)*, New York City, USA, 1–8.

Kashefipour, S. M., Lin, B., & Falconer, R. A. (2006). Modelling the fate of faecal indicators in a coastal basin. *Water Research*, *40*(7), 1413–1425.

Kay, D., Stapleton, C. M., Wyer, M. D., McDonald, A. T., Crowther, J., Paul, N., Jones, K., Francis, C., Watkins, J., Wilkinson, J., Humphrey, N., Lin, B., Yang, L., Falconer, R. A., & Gardner, S. (2005). Decay of intestinal enterococci concentrations in high-energy estuarine and coastal waters: Towards real-time T90 values for modelling faecal indicators in recreational waters. *Water Research*, *39*(4), 655–667.

Kim, M., Ligaray, M., Kwon, Y. S., Kim, S., Baek, S., Pyo, J., Baek, G., Shin, J., Kim, J., Lee, C., Kim, Y. M., & Cho, K. H. (2021). Designing a marine outfall to reduce microbial risk on a recreational beach: Field experiment and modeling. *Journal of Hazardous Materials*, *409*, 124587.

King, J., Ahmadian, R., & Falconer, R. A. (2021). Hydro-epidemiological modelling of bacterial transport and decay in nearshore coastal waters. *Water Research*, *196*(117049), 117049.

Li, G., Wang, B., Elliott, C. M., Call, B. C., Chapman, D. C., & Jacobson, R. B. (2022). A three-dimensional Lagrangian particle tracking model for predicting transport of eggs of rheophilic-spawning carps in turbulent rivers. *Ecological Modelling*, *470*, 110035.

Lin, B., Syed, M., & Falconer, R. A. (2008). Predicting faecal indicator levels in estuarine receiving waters—An integrated hydrodynamic and ANN modelling approach. *Environmental Modelling & Software*, *23*(6), 729–740.

Lubo, L., Phanikumar, M. S., Molloy, S. L., & Richard, L. W. (2006). Modeling the transport and inactivation of *E. coli* and Enterococci in the near-shore region of Lake Michigan. *Environmental Science & Technology*, *40*(16), 5022–5028.

Perkins, T. L., Perrow, K., Rajko-Nenow, P., Jago, C. F., Jones, D. L., Malham, S. K., & McDonald, J. E. (2016). Decay rates of faecal indicator bacteria from sewage and ovine faeces in brackish and freshwater microcosms with contrasting suspended particulate matter concentrations. *Science of the Total Environment*, *572*, 1645–1652.

Sagarduy, M., Courtois, S., Del Campo, A., Garmendia, J. M., & Petrau, A. (2019). Differential decay and prediction of persistence of Enterococcus spp. and *Escherichia coli* culturable cells and molecular markers in freshwater and seawater environments. *International Journal of Hygiene and Environmental Health*, *222*(4), 695–704.

Seo, J. Y., Choi, B.-J., Ryu, J., & Ha, H. K. (2022). Dynamic evolution of a secondary turbidity maximum under various forcing conditions in a microtidal estuary. *Marine Geology*, *446*, 106760.

Simantiris, N., Avlonitis, M., & Theocharis, A. (2022). Simulation of the transport of marine microplastic particles in the Ionian Archipelago (NE Ionian Sea) using a Lagrangian model and the control mechanisms affecting their transport. *Journal of Hazardous Materials*, *437*(129349), 129349.

Weiskerger, C. J., & Phanikumar, M. S. (2020). Numerical modeling of microbial fate and transport in natural waters: Review and implications for normal and extreme storm events. *Water*, *12*(7), 1876.

How to cite this article: Huang, G., Falconer, R., Lin, B., & Xu, C. (2022). Dynamic tracing of faecal bacteria processes from a river basin to an estuary using a 2D/3D model. *River*, 1–13. https://doi.org/10.1002/rvr2.27